5. Conclusions

We have shown that a conduction electron produces an autolocalized state in a wide range of values of the parameter $\alpha = t/J_{\rm ff}S^2$: the electron is localized in a ferromagnetic droplet of finite radius, embedded into an antiferromagnetic matrix. Therefore, the double-exchange model exhibits a strong tendency towards phase separation. It was also proved that the ferron state becomes unstable in the quantum case for small values of the parameter α, and the electron moves freely over the antiferromagnetic matrix with an effective hopping amplitude $t_{\rm eff} = t/\sqrt{2S+1}$. Our approach to the single-electron problem corresponds to low concentrations of charge carriers (for instance, holes in $La_{1-x}Ca_xMnO_3$). It is intimately related to the recent neutron experiments of Hennion's group on the experimental detection of small ferromagnetic droplets in an antiferromagnetic or canted matrix [15].

Employing the model of ferrons in an insulating matrix [13], we calculated the temperature and field dependences of magnetoresistance in manganites. In our earlier works we also found the expression for the resistance in the framework of the ferron model [13, 14]:

$$\rho = \frac{kT}{128\pi e^2 n^2 \omega_0 l^5} \exp\left(\frac{V}{2kT}\right), \tag{22}$$

where n is the ferron concentration. In recent experiments performed to measure the resistance in the optimal doping range [17–20] and at temperatures above $T_{\rm Curie}$(the paramagnetic phase), an exponential temperature dependence of resistance of the form $\rho \sim T\exp(V/2kT)$ was discovered, which is in qualitative agreement with formula (22) and confirms our ideas of the nature of charge transfer in the phase-separated domain.

Passing on to the analysis of magnetoresistance, we emphasize once again that it exhibits the following temperature and field dependence in small magnetic fields:

$$MR(H) = \frac{AH^2}{(kT)^2} + \frac{BH^2 H_{\rm a}}{(kT)^5}\,.$$

We note that such a dependence of magnetoresistance on the temperature and the external field was experimentally established by Babushkina's group [16] in $(La_{1-x}Pr_x)_{0.7}Ca_{0.3}MnO_3$ samples (see Fig. 3). In particular, in the strong-anisotropy case it was possible to observe the dependence of magnetoresistance of the form $MR(H) \sim \sim H^2/T^5$ derived theoretically in our work. Note that the expression for magnetoresistance (20) is rather general, depending only slightly on the specific model and operative even in the situation with many-electron ferromagnetic droplets [4, 21].

The authors wish to express their appreciation to D I Khomskiĭ, V I Marchenko, I A Fomin, B É Meĭerovich, I Gonzales, M Hennion, F V Kusmartsev, V L Aksenov, N A Babushkina, V V Moshchalkov, A N Taldenkov, and E Pchelkin for their helpful discussions. This work was supported by the Russian Foundation for Basic Research (grant Nos 02-02-16708 and 00-15-96570), INTAS grant No. 01-2008, and CRDF grant No. RP2-2355-MO-02.

References

1. Jin S et al. *Science* **264** 413 (1994)
2. Nagaev E L *Fizika Magnitnykh Poluprovodnikov* (Physics of Magnetic Semiconductors) (Moscow: Nauka, 1979) [Translated into English (Moscow: Mir Publ., 1983)]
3. Kasuya T *Solid State Commun.* **8** 1635 (1970)
4. Balagurov A M et al. *Phys. Rev. B* **64** 024420 (2001)
5. Krivoglaz M A *Usp. Fiz. Nauk* **111** 617 (1973) [*Sov. Phys. Usp.* **16** 856 (1974)]
6. Kagan M Yu, Kugel' K I *Usp. Fiz. Nauk* **171** 577 (2001) [*Phys. Usp.* **44** 553 (2001)]
7. Zener C *Phys. Rev.* **81** 440; **82** 403 (1951)
8. Anderson P W, Hasegawa H *Phys. Rev.* **100** 675 (1955)
9. de Gennes P-G *Phys. Rev.* **118** 141 (1960)
10. Nagaev É L *Usp. Fiz. Nauk* **166** 833 (1996) [*Phys. Usp.* **39** 781 (1996)]
11. Kagan M Yu, Khomskii D I, Mostovoy M V *Eur. Phys. J. B* **12** 217 (1999)
12. Pathak S, Satpathy S *Phys. Rev. B* **63** 214413 (2001)
13. Rakhmanov A L et al. *Phys. Rev. B* **63** 174424 (2001)
14. Sboychakov A O et al. *Zh. Eksp. Teor. Fiz.* **122** 869 (2002) [*JETP* **95** 753 (2002)]
15. Biotteau G et al. *Phys. Rev. B* **64** 104421 (2001)
16. Babushkina N A et al. *J. Phys.: Condens. Matter* **15** 259 (2003)
17. Babushkina N A et al. *Phys. Rev. B* **59** 6994 (1999)
18. Wagner P et al. *Europhys. Lett.* **58** 285 (2002)
19. Zhao J H et al. *Phys. Rev. B* **66** 184428 (2002)
20. Zhao J H et al. *J. Phys.: Condens. Matter* **13** 9349 (2001)
21. Uehara M et al. *Nature* **399** 560 (1999)

PACS numbers: **75.25.+z**, 75.47.Lx
DOI: 10.1070/PU2003v046n08ABEH001650

Neutron diffraction analysis of doped manganites

V L Aksenov, A M Balagurov, V Yu Pomyakushin

Doped manganites attract considerable attention from both theorists and experimenters in connection with the colossal magnetoresistance (CMR) effect observed in them. From the physical standpoint, manganites are of interest primarily due to an intimate connection between their electron, lattice, and spin subsystems. Recently, it has become evident that an important part in the physics of manganites is played by inhomogeneous states that show themselves, for instance, as the charge ordering of manganese cations, structural and magnetic polarons or a low-temperature phase separation. The employment of neutron diffraction analysis makes it possible to obtain detailed information on the crystal and magnetic structure of manganites, as well as to observe effects related to phase separation. The first neutron diffraction study of doped manganites was made even in the 1950s and reported in Ref. [1], which is regarded as a classical work concerned with the magnetic structure of $La_{1-x}Ca_xMnO_{3-\delta}$ compounds. It was found that there occur several different types of magnetic structures (seven types were proposed by Wollan and Koehler [1]), depending on the doping level and the oxygen stoichiometry, and, moreover, their superposition is also possible. Two mutually exclusive models were discussed for a long time to account for the simultaneous presence of diffraction peaks related to ferromagnetic (FM) and antiferromagnetic (AFM) order in the neutron diffraction patterns, which were observed in $LaMnO_{3-\delta}$ in Ref. [1] and later in other compounds (for instance, in $Pr_{0.7}Ca_{0.3}MnO_3$ [2]): the coexistence of two spatially separated magnetic (FM+AFM) phases, and a homogeneous state with a canted AFM structure. In the case of a mixed state, the question of characteristic inhomogeneity dimen-

sions remained unsolved. According to the theoretical estimates made in Nagaev's papers as far back as the 1970s (see his review [3] and references cited therein), the dimension of charge-separated domains is controlled by the Coulomb energy and cannot be large ($\leqslant 20$ Å), while the diffraction data suggest that the dimensions of, let us say, FM inclusions in the AFM matrix are no smaller than 1000 Å.

Beginning with the mid-1990s, a large number of neutron diffraction studies were performed, which bore witness to the existence of phase separation in doped manganites, both on microscopic (of the order of 10 Å) and mesoscopic (of the order of 1000 Å) scales of length. In particular, magnetic correlations and the long-wavelength spin dynamics in $La_{1-x}Ca_xMnO_3$ ($0 \leqslant x \leqslant 1/2$) compounds were studied by inelastic neutron scattering [4]. For $x = 1/3$, i.e., at the peak of magnetoresistance, at a temperature above 200 K (the ferromagnetic – paramagnetic phase transition temperature $T_C = 250$ K) observations were made of the development of critical spin fluctuations whose dimensions were estimated at about 12 Å up to T_C. A similar dimension of inhomogeneity domains was recorded for $x = 1/3$ with the aid of small-angle scattering for $T \geqslant T_C$ [5]. The coexistence of ferromagnetic and antiferromagnetic states was observed with the help of inelastic scattering in the vicinity of the central peak for the $La_{0.53}Ca_{0.47}MnO_3$ composition at $T = 0.93T_C$ [6]. Magnetic clusters or magnetic polarons typically measuring about 10 Å were also discovered in the antiferromagnetic state domain at a low doping level ($x = 0.05$ and 0.08) below T_N [7]. The above data testify to the occurrence of short-range order clusters measuring about 10 Å at different doping levels for $x < 0.5$. However, microscopic phase separation in the true sense of the word (see review [8]) can be spoken of with assurance only for low Ca concentrations ($x \leqslant 0.15$). The data of Refs [4, 5] are rather indicative of the presence of cluster precursors in the vicinity of the phase transition.

In a series of our works performed in 1998 – 2002, a detailed investigation was made into the $(La_{1-y}Pr_y)_{0.7}Ca_{0.3}MnO_3$ compound (hereafter referred to as LPCM-y), which is a typical representative of three-dimensional perovskite manganites [9 – 13]. It is interesting in that varying y from 0 to 1, which leads to a decrease in the average radius $\langle r_A \rangle$ of the A cation by only ~ 0.03 Å, proves to be sufficient for a radical change in the type of the magnetic structure and transport properties: the $La_{0.7}Ca_{0.3}MnO_3$ compound is a ferromagnetic metal below 250 K, and the $Pr_{0.7}Ca_{0.3}MnO_3$ compound is an insulator with a complex magnetic structure occurring below 150 K. It was in LPCM compounds that the giant isotope effect was discovered in 1998, which manifests itself when the metal state changes to the insulating one upon replacing the ^{16}O isotope with ^{18}O [14].

The $(La_{1-y}Pr_y)_{0.7}Ca_{0.3}MnO_3$ compounds were prepared at the Chemistry Department of Moscow State University in A R Kaul''s laboratory. The initial samples contained the natural mixture of oxygen isotopes (99.7% of ^{16}O). The samples were enriched with the ^{18}O isotope up to 85% in the Russian Research Centre 'Kurchatov Institute' (Moscow) in N A Babushkina's laboratory, where measurements were additionally made of their macroscopic characteristics (electrical conduction, magnetic susceptibility). Particular attention was given to oxygen stoichiometry: to account for the giant isotope effect observed in the LPCM-75 compound, a difference in isotope diffusion coefficients and the consequential difference in relative isotope content in the sample

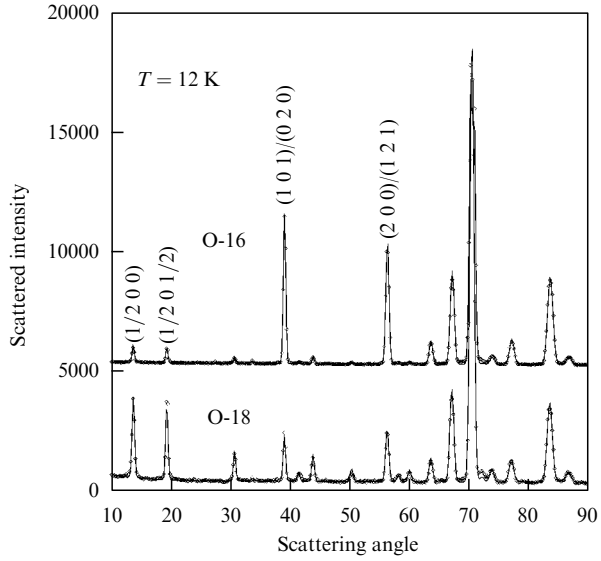

Figure 1. Diffraction spectra of samples with ^{16}O (O-16 upper) and ^{18}O (O-18 lower) isotopes, measured with the DMC at $T = 12$ K. For the O-16 spectrum, the ordinate axis scale is shifted by 5000 counts. The Miller indices mark the most intense FM and AFM peaks.

was assumed [15]. However, the data of both iodometric titration and diffraction analysis suggested that the isotopic substitution technique employed ensured the equality of oxygen content in the samples with ^{16}O and ^{18}O isotopes with the requisite accuracy (known to be better than 0.01). The neutron diffraction experiments were made in two neutron diffractometers: HRFD in the Joint Institute for Nuclear Research (Dubna) with a pulsed IBR-2 reactor, and DMC in the P Scherrer Institute with the SINQ source. In both cases, the diffraction spectra were measured in the sample warming mode from 10 to 293 K. An example of the diffraction spectrum measured in the DMC is given in Fig. 1 [11]. The refinement of the crystal and magnetic structures was performed by the Rietveld method in the Pnma space group which is conventional for manganites with $\langle r_A \rangle \approx 1.2$ Å, wherein the unit cell parameters are related to the parameter $a_c \approx 3.8$ Å of cubic perovskite in the following way: $a \approx c \approx \sqrt{2}\, a_c$, and $b \approx 2a_c$.

The LPCM-75 ($y = 0.75$) compound with the isotopes ^{16}O and ^{18}O was studied most extensively [10 – 12]. An analysis of the temperature dependence of the intensity of magnetic diffraction peaks showed that the sample with ^{18}O for $T \leqslant 145$ K exhibits superstructure reflections of the (0, 0, 1/2) and (1/2, 0, 1/2) types related to the establishment of antiferromagnetic order with a pseudo-CE type structure. Their intensity rises monotonically with decreasing temperature. The FM contribution to diffraction peaks was lacking to within the statistical accuracy achieved ($\sim 1.3\%$). For the sample with ^{16}O at the same $T_N \approx 145$ K there appears a pseudo-CE AFM structure, but the temperature dependence of the intensity is nonmonotonic with a maximum at $T \approx 110$ K, which correlates with the emergence of the FM component in the appropriate Bragg peaks. An obvious interpretation of this fact is the assumption of phase separation, namely, the emergence of FM-ordered domains and their gradual occupation of almost the entire sample volume (for $T \leqslant 50$ K, about 85% of the sample volume is ferromagnetically ordered). Precise structure analysis revealed that crystallographic parameters of the samples

with the ^{16}O and ^{18}O isotopes (unit cell parameters, interatomic distances, and valence angles) coincide with a high degree of precision throughout the temperature range above the transition point of ^{16}O sample to the FM phase. The structural identity of the samples for $T > T_{FM}$ and the smallness of structural changes in the ^{16}O-sample transition to the metallic state allowed the conclusion that structural effects are not the cause of their dramatically different behavior at low temperatures.

The coexistence of FM and AFM contributions to the diffraction peak intensities of the samples with ^{16}O isotopes was observed for all Pr concentrations greater than 0.6, but the character of the temperature dependence of AFM-peak intensities changed sharply in going from $y = 0.8$ to $y = 0.9$. In LPCM-80, the AFM peaks corresponding to the $\mathbf{k}_1 = (0\ 0\ 1/2)$ and $\mathbf{k}_2 = (1/2\ 0\ 1/2)$ propagation vectors emerge for $T_N \approx 130$ K, then the intensities of the peaks of both the types pass through a maximum for $T \approx T_C \approx 120$ K to decrease several-fold below 90 K. In LPCM-90, the intensities of the peaks of both the types gradually build up below $T_{AFM} \approx 130$ K and $T_{FM} \approx 95$ K without featuring the characteristic maximum observed for the compositions with $0.6 \leqslant y \leqslant 0.8$. This change in behavior could arise from the different degree of homogeneity of the low-temperature state. To gain direct information, we performed, following Ref. [1], experiments to study the effect of an external magnetic field on the magnetic structure of $(La_{1-y}Pr_y)_{0.7}Ca_{0.3}MnO_3$. The idea of this experiment is as follows: for a homogeneous state with a noncollinear magnetic structure, a simultaneous intensity variation of the diffraction peaks of various types should be observable, whereas for spatially separated FM- and AFM-ordered domains, one would expect a difference in the field strength that exerts a significant effect on the FM and AFM ordering. Experiments with the LPCM-75 and LPCM-90 samples were carried out in the DMC diffractometer using the geometry with a vertical, i.e., perpendicular to the scattering plane, direction of field in the range between 0 and 40 kOe at $T = 4.3$ K. Figure 2 shows the FM- and AFM-peak intensities as functions of the magnetic field strength [13]. One can see that the intensity of FM peaks for LPCM-75 (see Fig. 2a) increases linearly in the interval from 0 to 10 kOe, after which it remains practically constant. By contrast, the intensity of AFM peaks in this sample remains, to within the experimental error, invariable up to 10 kOe, following which it decreases to almost zero. It is evident that these dependences are impossible to explain in the framework of a homogeneous magnetic structure with a synchronous change of the FM and AFM components. For a compound with $y = 0.9$ (see Fig. 2b), a practically perfect correlation is observed for the changes in FM- and AFM-peak intensities: a linear (to within experimental errors) variation (the increase of FM peak intensity and the decrease of the AFM one), an abrupt jump between 25 and 30 kOe, and the attainment of saturation by 40 kOe.

Figure 3 displays the magnetic phase diagrams of $(La_{1-y}Pr_y)_{0.7}Ca_{0.3}MnO_3$ for the ^{16}O- and ^{18}O-bearing compounds, which were plotted employing the above results and some data available from the literature. One can see that both the diagrams are qualitatively similar, namely, the right lower part portrays a homogeneous FM-M state, and the left lower part a (nearly) homogeneous AFM-I state; the domain of a mixed two-phase state resides in between. The AFM-transition temperature depends only slightly on the Pr concentration, while T_{FM} decreases linearly with increasing y. There are

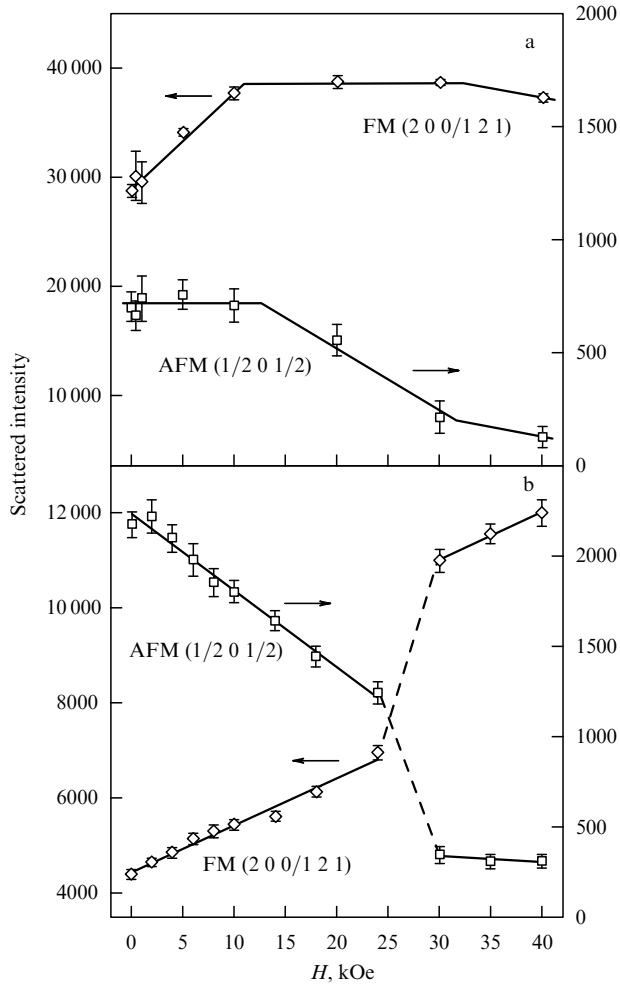

Figure 2. Intensities of the FM and AFM diffraction peaks for LPCM-75 (a) and LPCM-90 (b) samples as functions of the strength of external magnetic field, measured for $T = 4.3$ K. LPCM-75 resides in a spatially inhomogeneous two-phase state, so accordingly the variations of FM and AFM intensities are uncorrelated. By contrast, the greater part of the LPCM-90 sample is in a homogeneous state with a noncollinear magnetic structure. The synchronous variation of the FM and AFM intensities is related to the variation of the angle between the directions of magnetic moments of the neighboring Mn atoms.

also significant distinctions: the diagram for compounds with ^{18}O isotopes is shifted to the right, i.e., to the lower-y side, the two-phase domain is substantially narrower in y, the AFM structure is always collinear, i.e., the FM component is absent, and accordingly, there is no additional transition line below T_{AFM}; finally, the slope of the function $T_{FM}(y)$ is appreciably different (in compounds with ^{16}O isotopes, the temperature decreases slower with y). Furthermore, one can see that the AFM order appears only when $T_{AFM} \geqslant T_{FM}$. A similar behavior of the AFM and FM components was observed for other compounds experiencing the I – M transition, for instance, for $Pr_{0.65}(Ca_{0.7}Sr_{0.3})_{0.35}MnO_3$ [16]. The fact that the state emerging for a large y is not entirely homogeneous follows, in particular, from the behavior of the quantity $M = (\mu_{FM}^2 + \mu_{AFM}^2)^{1/2}$ — the total ordered magnetic moment of Mn [13]. In going from $y = 0.8$ to $y = 0.9$ in the samples with ^{16}O isotopes and from $y = 0.5$ to $y = 0.6$ in the samples with ^{18}O isotopes, the moment M decreases by $\sim 1/3$ in a jump-like manner (see Fig. 4). An estimate suggests that no more than 45% of the sample

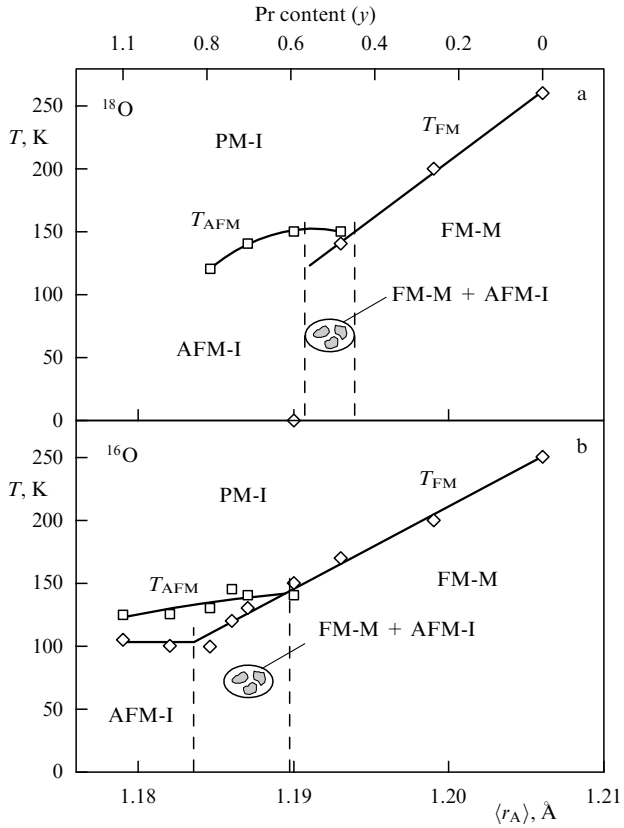

Figure 3. Magnetic phase diagram of LPCM-y with ^{18}O (a) and ^{16}O (b) isotopes (transition temperatures as functions of the average radius of an A-cation or the Pr content). Between the homogeneous ferromagnetic-metallic (FM-M) and the antiferromagnetic-insulating (AFM-I) states there lies a two-phase domain. The high-temperature state is paramagnetic-dielectric (PM-D). One can see that the diagram for the LPCM-y with the ^{18}O isotope is shifted to higher $\langle r_A \rangle$ in comparison with the diagram for the LPCM-y with the ^{16}O isotope.

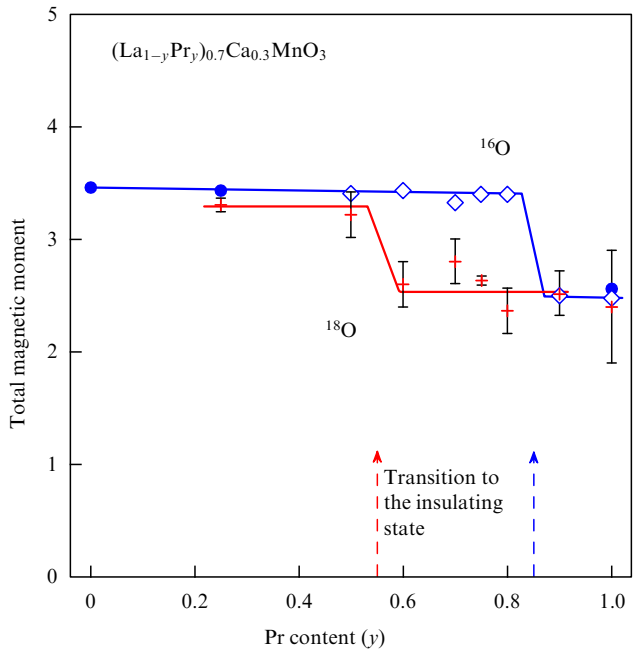

Figure 4. Total magnetic moment (in Bohr magnetons) of the LPCM-y with ^{16}O and ^{18}O isotopes as a function of Pr content. A sharp reduction of the moment corresponds to the transition of the samples to the (nearly) homogeneous insulating state.

volume resides in a magnetically ordered state in this case. This observation is consistent with the results of Ref. [17] obtained with the $Pr_{0.7}Ca_{0.3}MnO_3$ compound, wherein the existence of two crystalline phases was discovered. One of them may correspond to the domains in our samples that are in a magnetically disordered state.

As noted above, the issue of characteristic dimension of the occurring inhomogeneities is of paramount importance to the theoretical interpretation of the observed phase separation. An analysis of diffraction peak widths permits, at least, estimation of its lower bound at ~ 1500 Å. Such a high dimension of conducting and insulating domains calls for the search for stabilization mechanisms of the two-phase state, unrelated to charge segregation. One possible mechanism concerns the initial chemical inhomogeneity of the compounds under study (random substitutions of Ca or Pr for La), which is responsible for strong fluctuations in the probability of electron jumps into different positions. Monte Carlo simulations of this situation [18] revealed the emergence of giant metallic and dielectric clusters with characteristic dimensions of the order of $250a$, where $a \approx 4$ Å is the average distance between Mn atoms. Yet another possibility involves a crystallographic mechanism which implies a substantial difference in the atomic structures of coexistent phases. We performed a comparative structure analysis for $(La_{0.25}Pr_{0.75})_{0.7}Ca_{0.3}MnO_3$ samples enriched with the ^{16}O and ^{18}O isotopes, where for $T < 110$ K the former sample transformed to the mixed FM + AFM metallic state, and the latter sample remained insulating with a collinear AFM structure [12]. Our analysis produced direct evidence that the average values of the valence angles $\langle Mn-O-Mn \rangle$ and interatomic distances $\langle Mn-O \rangle$ are significantly different in the metallic and dielectric phases. The jump in unit cell volume ($\Delta V/V \approx -0.15\%$) resulting in this case is responsible for the occurrence of a stress field with a random orientation at the interfaces of coexistent phases. The corresponding change in free energy may be a factor stabilizing the two-phase state [19]. In the above-mentioned work [17], the high-resolution neutron diffraction and quasi-elastic neutron scattering techniques revealed phase separation in $Pr_{0.7}Ca_{0.3}MnO_3$ both at microscopic (5–20 Å) and mesoscopic (500–2000 Å) levels, and it was noted that mechanical deformations at the boundaries between metallic and dielectric domains may be the major driving force for the mesoscopic separation.

The similarity in phase diagrams for LPCM-y with ^{16}O and ^{18}O isotopes as regards their macroscopic properties was determined from the magnetic susceptibility measurement data in Ref. [20]. Diffraction data suggest that the phase diagrams are also similar in magnetic structure as well as mesoscopic properties (the degree of homogeneity of the ground state). The principal distinction is the shift of the phase diagram for LPCM-75 with the ^{18}O isotopes towards smaller y. Hence, it follows that the isotopic substitution did not result in the emergence of some fundamentally new state, but merely redistributed the energy balance. Indeed, the transition temperature to the ferromagnetic state is, according to the double-exchange model, proportional to the effective electron-hopping integral, which in turn depends on the average value of the valence angle $\langle Mn-O-Mn \rangle$ and (due to polaron renormalization) on the ion mass (see, for

instance, Ref. [21]):

$$T_{\mathrm{FM}} \sim t_{\mathrm{eff}} = t \exp\left(-\frac{E_{\mathrm{pol}}}{\hbar\omega}\right) \sim \sin\frac{\langle \mathrm{Mn-O-Mn}\rangle}{2} \exp\left(-\mathrm{const}\, M^{1/2}\right), \qquad (1)$$

where E_{pol} is the polaron shift energy, $\omega \sim \omega_{\mathrm{Debye}}$, and M is the ion mass. Hence, it is clear that compensating the reduction in T_{FM} with an increase in oxygen mass necessitates increasing the angle $\langle \mathrm{Mn-O-Mn}\rangle$, which can be attained by lowering y [12]. The relative changes of T_{FM} caused by these two factors can be compared when the constant in the exponential index is known. Agreement with experimental data on the shift, for instance, of the transition point from the pure FM state to the mixed FM + AFM state is reached for const ≈ 0.3. However, the functional dependences of the temperature difference ΔT_{FM} on y that follow from expression (1) and are observed in experiments for the compounds with ^{16}O and ^{18}O isotopes are inconsistent: ΔT_{FM} should increase with T_{FM} according to expression (1), but this temperature difference decreases according to both the magnetic and diffraction data. A plausible explanation of this effect, involving the assumption of a higher stability of polarons with ^{18}O isotopes, was put forward in Ref. [22].

The presently available comprehensive experimental material appears to be quite sufficient to arrive, relying on its theoretical analysis, at a definite conclusion as to what the cause of the CMR effect in manganites is. However, neutron diffraction investigations of isotope-enriched compounds bring up new questions, some of which are quite important. Why does the giant isotope effect manifest itself in a relatively broad range of variability of the average A-cation radius? What underlies the occurrence of the mesoscopically mixed state (in other words, why does the AFM – FM phase transition not proceed to completion)? Why does a significant volume fraction of the sample become magnetically disordered in the course of transition to the dielectric state? Why does the noncollinear AFM structure in LPCM-y with the ^{16}O isotope become collinear in LPCM-y with the ^{18}O isotope?

The authors express their gratitude to M Yu Kagan for helpful discussions, and to N A Babushkina, A R Kaul', and O Yu Gorbenko for fruitful cooperation. This work was supported by the Russian Federation Ministry of Industry and Science under State Contract No. 40.012.1.1.1148, the Russian Foundation for Basic Research (grant No. 03-02-16954), and INTAS (grant No. 01-2008).

References

1. Wollan E O, Koehler W C *Phys. Rev.* **100** 545 (1955)
2. Jirák Z et al. *J. Magn. Magn. Mater.* **53** 153 (1985)
3. Nagaev É L *Usp. Fiz. Nauk* **165** 529 (1995) [*Phys. Usp.* **38** 497 (1995)]
4. Lynn J W et al. *Phys. Rev. Lett.* **76** 4046 (1996)
5. De Teresa J M et al. *Nature* **386** 256 (1997)
6. Rhyne J J et al. *J. Appl. Phys.* **83** 7339 (1998)
7. Hennion M et al. *Phys. Rev. Lett.* **81** 1957 (1998)
8. Kagan M Yu, Kugel' K I *Usp. Fiz. Nauk* **171** 577 (2001) [*Phys. Usp.* **44** 553 (2001)]
9. Balagurov A M et al. *Pis'ma Zh. Eksp. Teor. Fiz.* **67** 672 (1998) [*JETP Lett.* **67** 705 (1998)]
10. Balagurov A M et al. *Pis'ma Zh. Eksp. Teor. Fiz.* **69** 46 (1999) [*JETP Lett.* **69** 50 (1999)]
11. Balagurov A M et al. *Phys. Rev. B* **60** 383 (1999)
12. Balagurov A M et al. *Eur. Phys. J. B* **19** 215 (2001)
13. Balagurov A M et al. *Phys. Rev. B* **64** 024420 (2001)
14. Babushkina N A et al. *Nature* **391** 159 (1998)
15. Nagaev E L *Phys. Rev. B* **58** 12242 (1998)
16. Yoshizawa H et al. *Phys. Rev. B* **55** 2729 (1997)
17. Radaelli P G et al. *Phys. Rev. B* **63** 172419 (2001)
18. Moreo A et al. *Phys. Rev. Lett.* **84** 5568 (2000)
19. Littlewood P *Nature* **399** 529 (1999)
20. Babushkina N A et al. *J. Phys.: Condens. Matter* **11** 5865 (1999)
21. Kugel' K I, Khomskiĭ D I *Zh. Eksp. Teor. Fiz.* **79** 987 (1980) [*Sov. Phys. JETP* **52** 501 (1980)]
22. Egami T, in *Localized to Itinerant Electronic Transition in Perovskite Oxides* (Structure and Bonding, Vol. 98, Ed. J B Goodenough) (Berlin: Springer-Verlag, 2001) p. 140

PACS numbers: 42.68.Bz, **42.79.–e**, 95.55.Cs
DOI: 10.1070/PU2003v046n08ABEH001653

Atmospheric adaptive optics

V P Lukin

1. Introduction

Research aimed at developing adaptive optical systems has been pursued in the Institute of Atmospheric Optics, Siberian Branch of the Russian Academy of Sciences (IAO, SB RAS) for more than 25 years. Traditional optical problems, namely, the problems of optical beam and image formation, are solved with the goal of providing:

— concentration of laser beam energy;
— improvement in the sharpness of an optical image;
— increase in the rate of data transmission in optical communication lines;
— fulfillment of several other specific requirements.

These problems are solved by adaptive optical – electronic systems by incorporating in their structure such new elements as:

— a wavefront corrector (an active optical element);
— a wavefront distortion sensor (a fluctuation meter);
— a reference source;
— a data processor and working algorithm.

Since these new elements (see Fig. 1), to say nothing of the system as a whole, are not commercially available, we had to

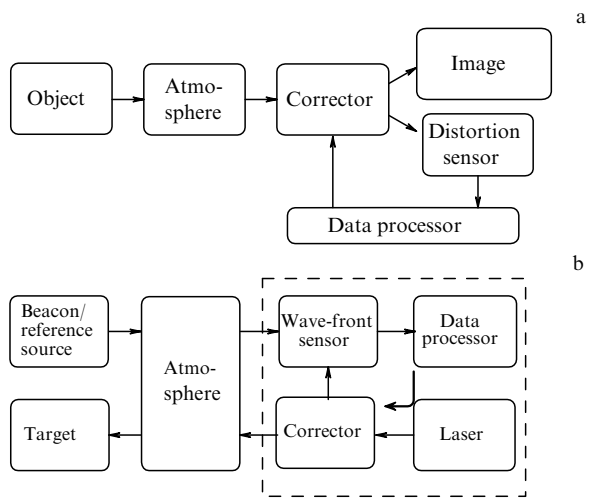

Figure 1. Atmospheric adaptive optical systems: (a) imaging, and (b) beaming.